Original Article

MOLECULAR METABOLISM

Wild-type IDH2 contributes to Epstein–Barr virus-dependent metabolic alterations and tumorigenesis

Feng Shi [1,2,3], Ya He [1,2,3], Jiangjiang Li [1,2,3], Min Tang [1,2,3,4], Yueshuo Li [1,2,3], Longlong Xie [1,2,3], Lin Zhao [1,2,3], Jianmin Hu [1,2,3], Xiangjian Luo [1,2,3,4], Min Zhou [1,2,3], Na Liu [1,2,3], Jia Fan [5], Jian Zhou [5], Qiang Gao [5], ShuangJian Qiu [5], Weizhong Wu [5], Xin Zhang [6], Weihua Jia [7], Ann M. Bode [8], Ya Cao [1,2,3,4,9,10,*]

ABSTRACT

Objective: Epstein–Barr virus (EBV) is a well-recognized oncogenic virus that can induce host cell metabolic reprogramming and tumorigenesis by targeting vital metabolic enzymes or regulators. This study aims to explore the role of wild-type isocitrate dehydrogenase 2 (IDH2) in metabolic reprogramming and tumorigenesis induced by EBV-encoded latent membrane protein 1 (LMP1).

Methods: Mechanistic dissection of wild-type IDH2 in EBV-LMP1-induced tumorigenesis was investigated using western blotting, real-time polymerase chain reaction (PCR), immunochemistry, chromatin immunoprecipitation (ChIP), and luciferase assay. The role of wild-type IDH2 was examined by cell viability assays/Sytox Green staining *in vitro* and xenograft assays *in vivo*.

Results: IDH2 over-expression is a prognostic indicator of poorer disease-free survival for patients with head and neck squamous cell carcinoma (HNSCC). IDH2 expression is also upregulated in nasopharyngeal carcinoma (NPC, a subtype of HNSCC) tissues, which is positively correlated with EBV-LMP1 expression. EBV-LMP1 contributes to NPC cell viability and xenograft tumor growth mediated through wild-type IDH2. IDH2-dependent changes in intracellular α-ketoglutarate (α-KG) and 2-hydroxyglutarate (2-HG) contribute to EBV-LMP1-induced tumorigenesis *in vitro* and *in vivo*. Elevated serum 2-HG level is associated with high EBV DNA and viral capsid antigen-immunoglobulin A (VCA-IgA) levels in patients with NPC. A significantly positive correlation exists between serum 2-HG level and regional lymph node metastases of NPC. EBV-LMP1 enhances the binding of c-Myc with the *IDH2* promoter and transcriptionally activates wild-type IDH2 through c-Myc. Targeting IDH2 decreased intracellular 2-HG levels and survival of EBV-LMP1-positive tumor cells *in vitro* and *in vivo*.

Conclusions: Our results demonstrate that the EBV-LMP1/c-Myc/IDH2^{WT} signaling axis is critical for EBV-dependent metabolic changes and tumorigenesis, which may provide new insights into EBV-related cancer diagnosis and therapy.

Keywords Epstein-Barr virus; Tumorigenesis; Metabolic reprogramming; Isocitrate dehydrogenase 2; Nasopharyngeal carcinoma

1. INTRODUCTION

Oncogenic viral infection is an important risk factor for infection-related cancers [1]. Epstein–Barr virus (EBV) is a well-recognized oncogenic virus that is closely associated with a number of human malignancies. Among these, nasopharyngeal carcinoma (NPC), a distinctive histological subtype of head and neck squamous cell carcinoma (HNSCC), is one of the most common EBV-related malignancies [2]. EBV-encoded latent membrane protein 1 (EBV-LMP1) is a driving oncogene in NPC and plays a major role in promoting almost all hallmarks of cancer [3,4].

The mitochondrial reduced nicotinamide adenine dinucleotide phosphate (NADPH)-dependent isocitrate dehydrogenase 2 (IDH2) is a key enzyme in the tricarboxylic acid (TCA) cycle that reversibly catalyzes isocitrate to α-ketoglutarate (α-KG). Gain-of-function mutation of IDH2 results in the accumulation of the onco-metabolite 2-hydroxyglutarate (2-HG), which is a competitive inhibitor of α-KG-dependent dioxygenases [5]. Although IDH2 mutation has been extensively described in multiple cancers, especially in glioma and

[1]Key Laboratory of Carcinogenesis and Invasion, Chinese Ministry of Education, Department of Radiology, Xiangya Hospital, Central South University, Changsha 410078, China [2]Cancer Research Institute and School of Basic Medical Science, Xiangya School of Medicine, Central South University, Changsha 410078, China [3]Key Laboratory of Carcinogenesis, Chinese Ministry of Health, Changsha 410078, China [4]Molecular Imaging Research Center of Central South University, Changsha 410008, Hunan, China [5]Key Laboratory for Carcinogenesis and Cancer Invasion, Chinese Ministry of Education, Zhongshan Hospital, Shanghai Medical School, Fudan University, Shanghai 200000, China [6]Department of Otolaryngology Head and Neck Surgery, Xiangya Hospital, Central South University, Changsha 410078, China [7]State Key Laboratory of Oncology in South China, Sun Yat-sen University Cancer Center, Guangzhou 510060, China [8]The Hormel Institute, University of Minnesota, Austin, MN 55912, USA [9]Research Center for Technologies of Nucleic Acid-Based Diagnostics and Therapeutics Hunan Province, Changsha 410078, China [10]National Joint Engineering Research Center for Genetic Diagnostics of Infectious Diseases and Cancer, Changsha 410078, China

*Corresponding author. Key Laboratory of Carcinogenesis and Invasion, Chinese Ministry of Education, Department of Radiology, Xiangya Hospital, Central South University, Changsha 410078, China. E-mail: ycao98@vip.sina.com (Y. Cao).

Received January 13, 2020 • Revision received February 11, 2020 • Accepted February 11, 2020 • Available online 18 February 2020

https://doi.org/10.1016/j.molmet.2020.02.009

leukemia, the mutation is rare in other types of cancers. Recently, the significance of aberrant expression of wild-type IDH2 has been recognized in cancers. IDH2 expression is upregulated in esophageal squamous cell carcinoma, thyroid cancer, lung cancer, and breast cancer, and downregulated in hepatocellular carcinoma, melanomas, and gastric cancer [6]. Investigation of somatic mutations in the cBioPortal database did not demonstrate any evidence for IDH2 mutation in NPC. We previously showed that wild-type IDH2 overexpression decreased α-KG levels and induced high 2-HG levels and the Warburg effect, which contributes to cell survival and tumor growth in lung cancer [7].

EBV-LMP1 can induce host cell metabolic reprogramming and tumorigenesis by targeting vital metabolic enzymes or regulators, such as hexokinase 2 (HK2), lactic dehydrogenase A (LDHA), fumarate hydratase (FH), adenosine 5′ monophosphate-activated protein kinase (AMPK), c-Myc, and hypoxia-inducible factor 1 alpha (HIF-1α) [8–11]. Here, we evaluated the role of wild-type IDH2 in metabolic reprogramming and tumorigenesis induced by EBV-LMP1. Based on the present study, we considered wild-type IDH2 to be a novel downstream effector of EBV-LMP1 and a potential therapeutic target for EBV-related cancers.

2. MATERIALS AND METHODS

2.1. Clinical specimens

Nasopharyngitis and NPC tissues were collected from the Department of Pathology at Xiangya Hospital, Central South University, Changsha, China. Serum samples from patients with NPC were obtained from Sun Yat-Sen University Cancer Center, Guangzhou, China. All patients signed informed consent forms for sample collection. All clinical data were obtained from the hospital pathologic records. The study was approved by the Medical Ethics Committee of Xiangya Hospital, Central South University (No. 201803134).

2.2. Detection of EBV DNA copy number and VCA-IgA antibody in serum

EBV DNA copy number analysis was conducted as described previously [12]. Immunoglobulin A antibody titers against EBV viral capsid antigen (VCA-IgA) in serum were measured using a commercial kit (Cat: C-0396, Tarcine, Beijing, China).

2.3. Cell culture

The human NPC cell lines, HK1, HK1-LMP1, HNE2, and HNE2-LMP1 have been described previously [8,13]. NPC cell lines were cultured in Roswell Park Memorial Institute (RPMI)-1640 medium (Cat: 11875500, Gibco, Grand Island, NY, USA) supplemented with 10% fetal bovine serum (FBS; Cat: 04-001-1, BI, Kibbutz Beit-Haemek, Israel) at 37 °C in 5% CO_2.

Cells were transfected with siRNA or plasmid vectors using Lipomax (Cat: 32012, Sudgen, Nanjing, China) according to the manufacturer's instructions. The small interfering RNA (siRNA) target sequences and plasmid constructs are described in the Supplementary Materials and Methods.

2.4. Reagents and antibodies

Dimethyl sulfoxide (DMSO) was obtained from Sigma–Aldrich (Cat: D2650, St. Louis, MO, USA). Octyl-α-ketoglutarate (octyl-α-KG) and octyl-α-hydroxyglutarate (octyl-2-HG) were from Cayman (Cat: 11970 and 16366, Ann Arbor, MI, USA). AGI-6780 and MG132 were purchased from MedChemExpress (Cat: HY-15734 and HY-13259, Monmouth Junction, NJ, USA).

The following antibodies were used: mouse anti-IDH2 (Cat: ab55271, Abcam, Cambridge, MA, USA), mouse anti-β-actin (Cat: A5441, Sigma), rabbit anti-LMP1 (Cat: ab78113, Abcam), rabbit anti-IDH1 (Cat: ab172964, Abcam), and mouse anti-c-Myc (Cat: sc-40, Santa Cruz, Dallas, TX, USA).

The expression vectors for IDH2 and LMP1 have been described previously [7,14].

2.5. Immunohistochemistry (IHC)

IHC analysis was conducted as described previously [15]. IHC staining was scored blindly with no information on the clinical data provided.

2.6. Western blotting

Western blot analysis was conducted as previously described [9]. Because of the rapid degradation of the LMP1 protein, cells were incubated with 10 mM MG132 for 6 h before harvest to accumulate LMP1 for detection [16].

2.7. RNA isolation and real-time PCR

Total mRNA was isolated using the NucleoZOL reagent (Cat: 740404, MACHEREY- NAGEL GmbH & Co. KG, Düren, Germany). The RevertAid First Strand cDNA Synthesis Kit (Cat: K1622, Invitrogen, Carlsbad, CA, USA) was used for reverse transcription. Real-time polymerase chain reaction (PCR) analysis was performed in triplicate using the SYBR™ Green Master Mix (Cat: A25742, Invitrogen) on the ABI7500 Real-Time System (Applied Biosystems). The primers are listed in the Supplementary Materials and Methods.

2.8. Cell viability assay

Cells were seeded on 96-well plates in triplicate. The Cell Counting Kit-8 (Cat: CK04, Dojindo, Tabaru, Japan) was used to evaluate viability. Absorbance was measured at a wavelength of 450 nm using the BioTek Elx800 microplate reader.

2.9. Cell death assay

The cell death assay was performed by using Sytox Green (Cat: S34860, Invitrogen). Cells were incubated with 30 nM Sytox Green for 20 min in the dark at room temperature, and then visualized with the Leica DMI3000 fluorescence microscope.

2.10. α-KG and 2-HG assays

Intracellular α-KG and 2-HG were measured using the alpha-ketoglutarate colorimetric fluorometric assay kit and D-2-hydroxyglutarate colorimetric assay kit (Cat: K677 and K213, Biovision, Milpitas, CA, USA), respectively. The level of 2-HG in the serum was measured using the PicoProbe™ D-2-hydroxyglutarate assay kit (Cat: K970, Biovision).

2.11. Database analysis

The cBioPortal for the Cancer Genomics Database can be acquired online (http://www.cbioportal.org/index.do). The TCGA dataset ($N = 530$) was used to analyze the prognostic value of IDH2 in HNSCC.

2.12. Tumorigenicity assay

This study was approved by the Medical Ethics Committee (for experimental animals) of Xiangya Hospital, Central South University (No. 201803135). The analysis was performed as described previously [17]. To examine the effect of IDH2 on LMP1-induced tumorigenesis, cells (HNE2-LMP1-scramble or HNE2-LMP1-shIDH2, 3×10^6 per mouse) were injected subcutaneously into the flank regions of 6-week-

old female BALB/c-nu mice. The weight of mice and tumor volume were measured twice a week. The tumor volume was calculated using the following formula: $V = 1/6\pi \times \text{length} \times \text{width}^2$. The mice were euthanized after 5 weeks, and the weight of xenograft tumors was obtained at the same time.

To evaluate the anticancer effect of AGI-6780, HNE2-LMP1 cells (3×10^6 per mouse) were injected subcutaneously into the flank regions of 6-week-old female BALB/c-nu mice. When tumors reached a volume of approximately 100–150 mm^3, mice were divided randomly into two groups. The mice were treated repeatedly with intraperitoneal injections of corn oil (vehicle) or AGI-6780 (150 mg/kg) twice a week for seven doses, respectively. The weights of mice and tumor volume were measured at the time of each injection. The average weight of tumor tissues was obtained when the mice were euthanized.

2.13. Luciferase assay

The luciferase reporter assays were performed in triplicate using the Dual-Luciferase Reporter Assay System (Cat: E1910, Promega, Madison, WI, USA). The transfection efficiency was measured by co-transfection with the *Renilla* luciferase expression plasmid, pRL-SV40. The data are presented as the ratio of firefly luciferase activity to *Renilla* luciferase activity.

2.14. Chromatin immunoprecipitation (ChIP) assay

The analysis was performed as described previously [18]. Chromatin samples were immunoprecipitated with either anti-c-Myc or mouse immunoglobulin G (IgG) as a negative control. Precipitated DNA was amplified by PCR using primers listed in Supplementary Materials and Methods. Non-immunoprecipitated chromatin fragments were used as an input control.

2.15. Statistical analysis

All statistical analyses were performed using SPSS 17.0 software. The experimental results were statistically evaluated by the Student t test, the Pearson chi-square test, the Spearman rank correlation coefficient, the analysis of variance (ANOVA) test, Cox regression analysis, and Kaplan–Meier analysis. A value of $p < 0.05$ was considered statistically significant.

3. RESULTS

3.1. IDH2 is a prognostic indicator of poorer disease-free survival in patients with HNSCC

Using genomic analysis of *IDH2* in the cBioPortal database, genetic alterations were found in only 7 of 1611 samples in seven HNSCC datasets (Figure S1). The mRNA expression of *IDH2* was significantly increased in HNSCC tissues compared with normal tissues from the online GENT database, suggesting that over-expression of *IDH2* is the main alteration in HNSCC rather than genetic alterations (Figure 1A). Next, we analyzed *IDH2* expression in different stages of HNSCC in patients from the TCGA database. The results showed that *IDH2* expression was positively related with tumor size (T stage), regional lymph node metastases (N stage), and advanced clinical stage (Figure 1B–D). The survival analysis showed that patients with low expression of *IDH2* had longer disease-free survival compared with those with high *IDH2* expression ($N = 392$; accumulative probability of survival $> 50\%$ vs. median survival time of 49.97 months, Figure 1E). Cox regression analysis indicated that lymph node metastasis, advanced clinical stage, and high *IDH2* expression were significantly correlated with poorer disease-free survival (Table S1).

3.2. IDH2 is over-expressed in NPC tissues

Similarly in NPC, a subtype of HNSCC, no genetic alterations were found from the cBioPortal database (Figure S1). We also confirmed that no hotspot mutations of IDH1 (R132) or IDH2 (R140/R172) were found in NPC cells in this study (Figure S2). However, IHC analysis showed that the level of IDH2 protein expression was higher in NPC than that in nasopharyngitis (NP) tissues (Figure 2A). Also, IDH2 expression in NPC cell lines (HNE2, HK1, HK1-EBV, HONE1, HONE1-EBV, C666-1) was higher than that in the immortalized nasopharyngeal epithelial cell line (NP460) (Figure S3).

3.3. EBV-LMP1 promotes wild-type IDH2 expression

Considering EBV-LMP1 to be a driving oncogene of NPC, we evaluated the expression of EBV-LMP1 and IDH2 by IHC in consecutive sections of NPC tissues (Figure 2B). By the Spearman rank correlation coefficient, a significantly positive correlation was found between EBV-LMP1 and IDH2 expression (Table S2). To determine whether LMP1 promotes IDH2 expression in NPC cells, we analyzed expression in two NPC cell lines with wild-type IDH1/2 and stable expression of LMP1. We observed that IDH2 mRNA, protein expression, and enzyme activity were increased in LMP1-expressing cell lines (HK1-LMP1 and HNE2-LMP1) compared with their parental cells (HK1 and HNE2), whereas IDH1 protein expression was not significantly changed (Figure 2C–D and Figure S4-6). Knockdown of LMP1 in LMP1-expressing cell lines led to a decrease in IDH2 expression and enzyme activity (Figure S5-6). IDH2 expression was also upregulated in LMP1 transiently transfected NPC cells (Figure 2E and Figure S7). The knockdown of LMP1 in HK1-EBV and HONE1-EBV decreased IDH2 expression (Figure S8). These data suggest that EBV-LMP1 could upregulate wild-type IDH2 expression in NPC cells.

3.4. Wild-type IDH2 plays a key role in EBV-LMP1-induced tumorigenesis

Our previous studies showed that wild-type IDH2 promoted tumor growth in lung cancer and EBV-LMP1 enhanced survival and proliferation of NPC cells [7,19,20]. In the present study, we also confirmed that LMP1 increased NPC cell viability (Figure S9). Thus, we wondered whether IDH2 contributed to LMP1-induced cell survival. Using a lentivirus strategy, LMP1-negative NPC cells stably over-expressing IDH2 (HK1-IDH2 and HNE2-IDH2) and LMP1-positive NPC cells with stable knockdown of IDH2 (HK1-LMP1-shIDH2-1/2 and HNE2-LMP1-shIDH2-1/2) were generated and IDH2 expression was confirmed by western blot analysis (Figure 3A). IDH2 over-expression enhanced the viability of NPC cells (Figure 3B). The knockdown of IDH2 decreased viability and increased death of LMP1-expressing NPC cells (Figure 3C–D). To further examine the effect of IDH2 on LMP1-induced tumorigenesis, we performed a xenograft tumor growth assay in which HNE2-LMP1 or HNE2-LMP1-shIDH2-1 cells were injected subcutaneously into nude mice. The tumor volume and weight from the HNE2-LMP1-shIDH2-1 group were significantly lower compared with the HNE2-LMP1 group (Figure 3E–F). LMP1 and IDH2 expression in xenograft tumors was confirmed by IHC (Figure S10). These findings indicate that EBV-LMP1 contributes to NPC cell survival *in vitro* and xenograft tumor growth *in vivo* mediated through wild-type IDH2.

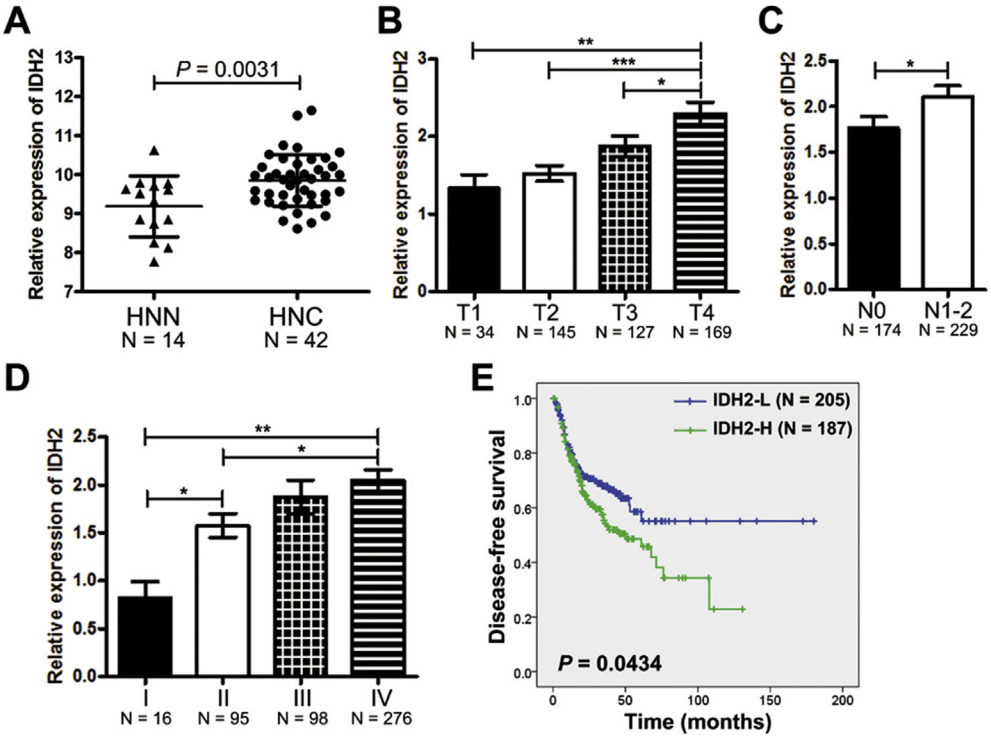

Figure 1: IDH2 over-expression in HNSCC. A, IDH2 expression in HNSCC tissues (HNC, N = 42) and normal tissues (N = 14) from the online GENT database. IDH2 expression was compared among different stages of B, pathologic T stage, C, regional lymph node metastases N stage, and D, AJCC clinical stage in patients with HNSCC from the TCGA database. E, Kaplan—Meier survival curves of patients with HNSCC with IDH2 expression from the TCGA database. Data are presented as means ± S.D.; *, $p < 0.05$; **, $p < 0.01$; ***, $p < 0.001$.

3.5. EBV-LMP1 promotes the production of 2-HG and decreases intracellular α-KG concentration

We have recently shown that intracellular 2-HG was increased in EBV-infected NPC cell lines [10]. In the present study, we examined the level of 2-HG in serum from patients with NPC. The concentration of 2-HG was significantly increased in the EBV DNA-high copy group and was also positively associated with the level of VCA-IgA (Figure 4A), suggesting that EBV infection was associated with increased serum 2-HG level. Further analysis showed that the level of serum 2-HG was significantly increased in patients with a high degree of regional lymph node metastases (N2—N3) compared with patients in early stages (N0—N1, Figure 4B). Consistent with the present results and our previous study [10], LMP1-positive NPC cells showed significant increases in intracellular 2-HG levels and decreases in α-KG levels (Figure 4C).

3.6. Over-expression of wild-type IDH2 is responsible for EBV-LMP1-dependent metabolic changes and tumorigenesis

Considering results of our previous studies in lung cancer [7], we hypothesized that wild-type IDH2 might be responsible for EBV-LMP1-modulated metabolic changes. The effect of IDH2 on the level of intracellular 2-HG and α-KG was confirmed first in NPC cells. Results indicated that the intracellular α-KG levels were significantly decreased in IDH2 over-expressing NPC cells, whereas the 2-HG levels were increased (Figure 4D). Knockdown of IDH2 in LMP1-positive NPC cells enhanced the intracellular α-KG levels and led to a decrease in 2-HG levels (Figure 4E). Furthermore, the levels of α-KG were higher in xenograft tissues from mice inoculated with HNE2-LMP1-shIDH2-1-expressing cells compared with levels in mice inoculated with HNE2-LMP1 cells (Figure 4F). In contrast, the 2-HG levels were lower in the HNE2-LMP1-shIDH2-1 group (Figure 4F). These data suggest that IDH2 plays a critical role in EBV-LMP1-dependent metabolic changes.

To further confirm the effect of metabolic changes on cell viability, cell-permeable octyl-α-KG and octyl-2-HG, respectively, were added to the culture medium. Octyl-2-HG treatment enhanced viability of LMP1-negative NPC cells, whereas incubation with octyl-α-KG diminished viability of LMP1-positive NPC cells (Figure 4G—H). In EBV-positive NPC cells (HK1-EBV), knockdown of LMP1 decreased cell viability. Octyl-2-HG treatment could partly rescue cell viability (Figure S11). Overall, these results indicate that IDH2-dependent changes in intracellular α-KG and 2-HG contribute to EBV-LMP1-induced tumorigenesis.

3.7. EBV-LMP1 facilitates *IDH2* transcription mediated through c-Myc

EBV-LMP1 significantly promoted *IDH2* mRNA and protein expression (Figure 2C—E), suggesting that IDH2 is regulated at the transcriptional level. Using online database searching (www.cbrc.jp/research/db/TFSEARCH), two putative c-Myc-binding sites were found in the *IDH2* promoter (Figure S12). c-Myc is a well-known master regulator of metabolic reprogramming and also an important transcriptional factor mediated by LMP1 [8]. The protein expression and transcriptional activity of c-Myc were obviously upregulated in LMP1-positive NPC cells (Figure S13 and Figure 5A). From the online database analysis, *c-Myc* expression was substantially increased in NPC tissues compared with nasopharynx tissues, and moreover, mRNA expression of *c-Myc* was significantly and positively associated with the expression of *IDH2* (Figure S14). The expression of c-Myc and IDH2 was evaluated by IHC in

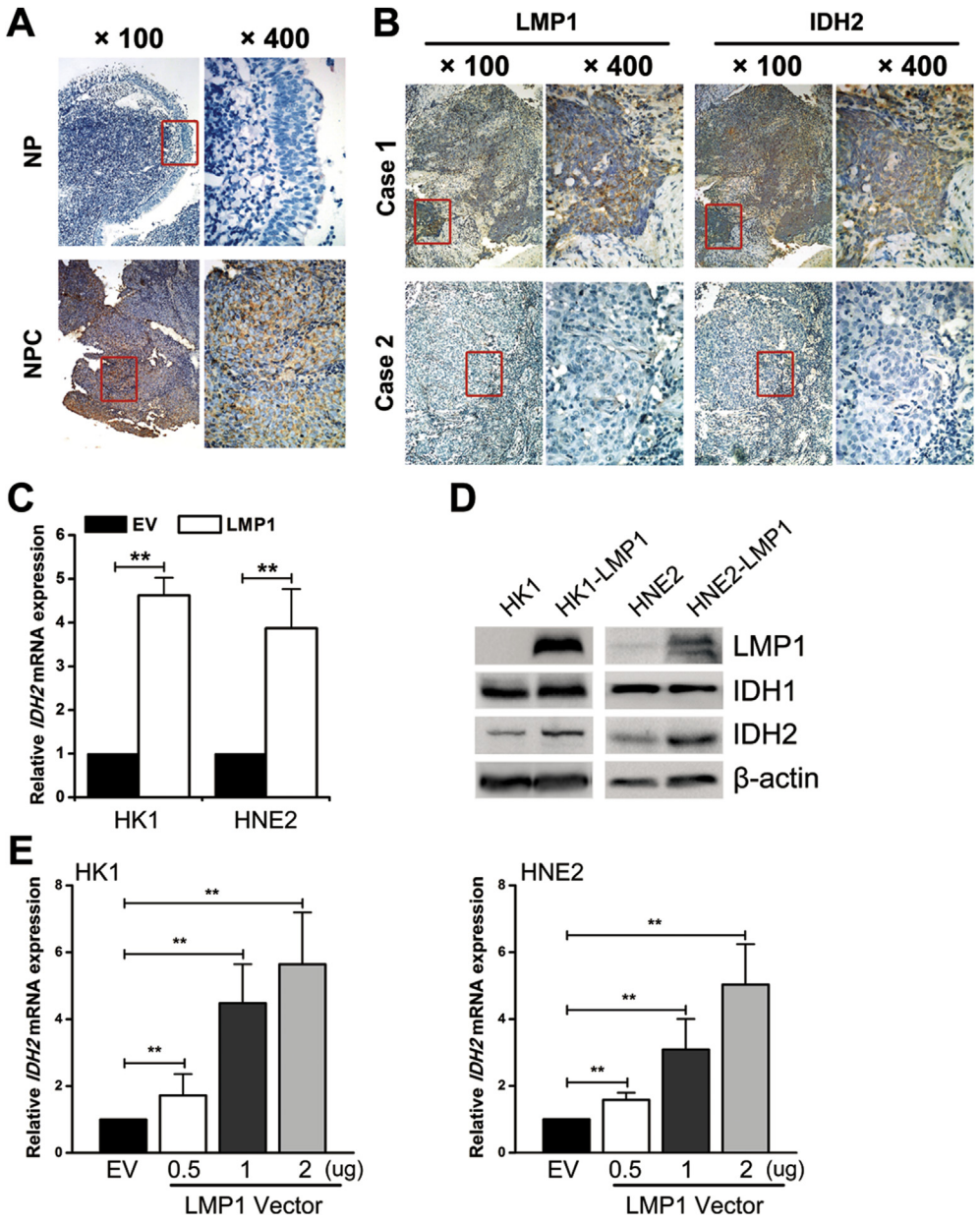

Figure 2: EBV-LMP1 promotes wild-type IDH2 overexpression in NPC. A, representative IHC photos for the expression of IDH2 in nasopharyngitis (NP) and nasopharyngeal carcinoma (NPC) tissues. B, representative IHC photos for the expression of LMP1 and IDH2 in consecutive sections of NPC tissues. C, *IDH2* mRNA expression was determined by RT-PCR (columns = mean; bars = S.D.; N = 3; **, $p < 0.01$). D, LMP1, IDH1, IDH2 protein expression was detected by western blot analysis, and β-actin served as a loading control. E, HK1 *(left)* and HNE2 *(right)* cells were transiently transfected with 0.5, 1, and 2 μg of LMP1 vector. *IDH2* mRNA expression was determined by RT-PCR (columns = mean; bars = S.D.; N = 3; **, $p < 0.01$).

NPC tissues. The representative images are shown in supplementary figure S15. By the Spearman rank correlation coefficient, a significantly positive correlation was found between c-Myc and IDH2 expression (Table S3). We also confirmed that no hotspot mutations of c-Myc (Thr58 and Ser62) were found in NPC cells in this study (Figure S16).

To determine whether c-Myc is involved in EBV-LMP1-dependent upregulation of IDH2, c-Myc was knocked down in LMP1-positive NPC cells. The results indicated that *IDH2* mRNA and protein expression were decreased in LMP1-positive NPC cells transfected with *c-Myc* siRNA (Figure 5B–C), suggesting that c-Myc might be a transcriptional factor for IDH2. To test this idea, the ChIP assay was performed with two pairs of primers that covered the two potential c-Myc-binding sites (Figure S12). The data showed that c-Myc could directly bind to the *IDH2* promoter, whereas the binding of the −1730 bp to −1416 bp region (c-Myc-binding site #2) was enhanced by LMP1 (Figure 5D and Figure S12). We then generated a luciferase reporter vector with an IDH2 promoter fragment (−1733 bp to −1266 bp, pGL3-IDH2). The luciferase activity significantly increased in LMP1-positive NPC cells compared with their parental cells (Figure 5E). Knockdown of *c-Myc* by siRNA diminished the luciferase activity in LMP1-positive NPC cells (Figure 5F). Furthermore, deletion of the c-

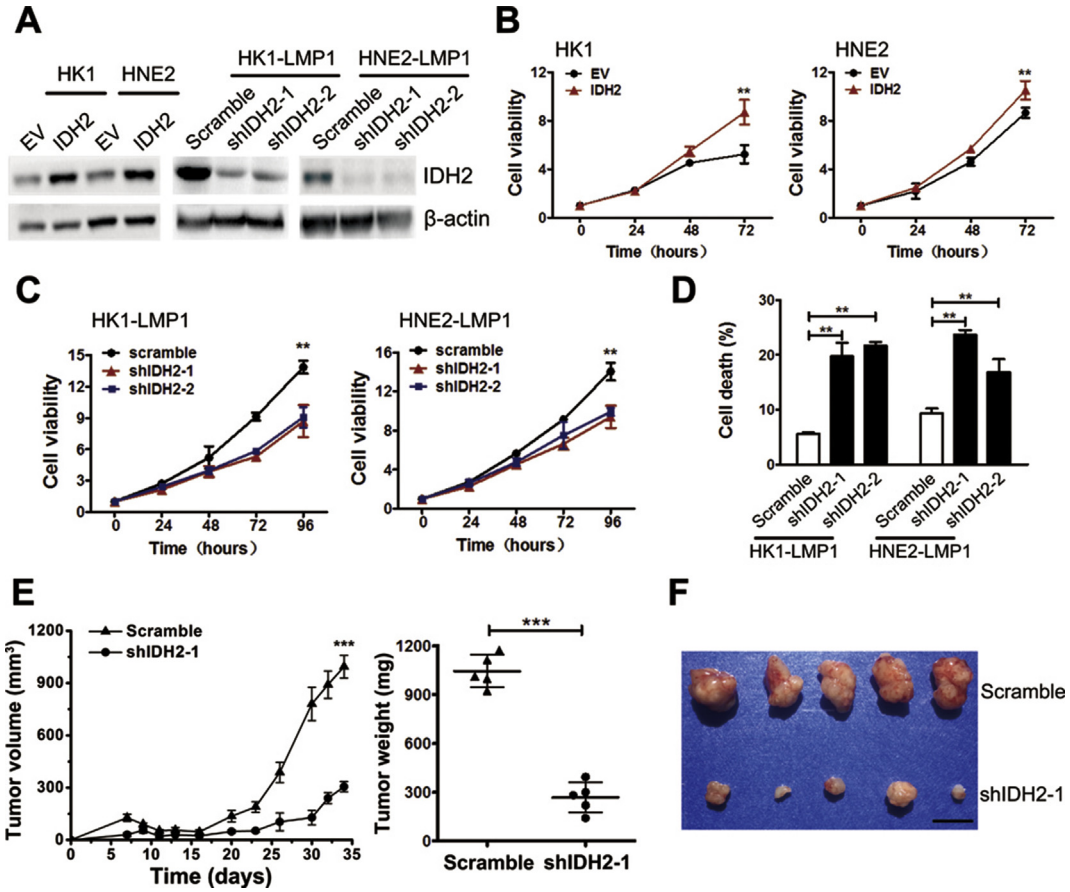

Figure 3: Wild-type IDH2 plays a key role in EBV-LMP1-induced tumorigenesis. A, IDH2 protein expression was detected by western blot analysis. EV, empty vector. B, cell viability was measured in empty vector- or IDH2-overexpressing cells using the MTS assay. C, viability was measured in cells transfected with scramble or IDH2 shRNA using the MTS assay. D, cell death was measured by Sytox Green staining in groups as indicated. E, tumor volume and weight were measured in xenografts in mice inoculated with HNE2-LMP1 cells transfected with scramble or IDH2 shRNA-1 (N = 5). F, photographs of xenograft tumors are shown (scale bar = 1 cm). Data are presented as means ± S.D.; **, $p < 0.01$; ***, $p < 0.001$.

Myc-binding site #2 (−1446 bp to −1437 bp) from pGL3-IDH2 (pGL3-IDH2-mut) led to a significant decrease of luciferase activity (Figure 5G). These results demonstrate that c-Myc is a transcriptional factor for IDH2 and that LMP1 could facilitate the regulation by enhancing the binding of c-Myc with the −1446 bp to −1437 bp region in the *IDH2* promoter.

3.8. c-Myc enhances EBV-LMP1-induced metabolic changes and tumorigenesis

We next examined the effect of c-Myc on LMP1-dependent tumorigenesis. Viability was inhibited in LMP1-positive NPC cells transfected with *c-Myc* siRNAs (Figure 5H). Furthermore, knockdown of c-Myc led to a decrease in intracellular 2-HG levels and an increase in α-KG levels (Figure 5I—J). These results suggest that c-Myc is critical in LMP1-dependent tumorigenesis.

3.9. Targeting EBV-LMP1-induced wild-type IDH2 over-expression inhibits cell viability and tumor growth

Because IDH2 is a critical downstream effector of EBV-LMP1-induced tumorigenesis (Figure 7), we wondered whether IDH2 could be a therapeutic target for EBV-LMP1-positive tumors. We previously showed that AGI-6780, a pharmacological inhibitor of the IDH2 enzyme, decreased IDH2 activity and viability of wild-type IDH2 lung cancer cells [7]. Consistently, we confirmed that AGI-6780 treatment decreased IDH2 activity and intracellular 2-HG levels in LMP1-positive NPC cells (Figure 6A—B). AGI-6780 inhibited NPC cell viability in a dose- and time-dependent manner. Interestingly, LMP1-positive cells were more sensitive to AGI-6780 (Figure 6C—D). Moreover, the percentage of dead cells increased with AGI-6780 treatment (Figure 6E). We further evaluated the anticancer effect of AGI-6780 in a xenograft tumor assay. The tumor volume and weight from the AGI-6780-treated group were significantly lower compared with the vehicle group (Figure 6G). No obvious difference was observed in body weight of mice between the two groups (Figure S17). The intracellular 2-HG levels were also lower in xenograft tissues from the AGI-6780-treated group (Figure 6F). These results suggest that inhibition of IDH2 decreased viability *in vitro* and xenograft tumor growth *in vivo* of EBV-LMP1-positive tumor cells.

4. DISCUSSION

Many eukaryotic viruses can modify host cellular metabolism to ensure their replication and spread, whereas metabolic reprogramming may be conducive to the survival of infected cells [21,22]. We have previously shown that the oncogenic virus EBV enhances aerobic glycolysis (i.e., Warburg effect), inhibits mitochondrial oxidative phosphorylation, and causes abnormal alterations in multiple metabolites by regulating

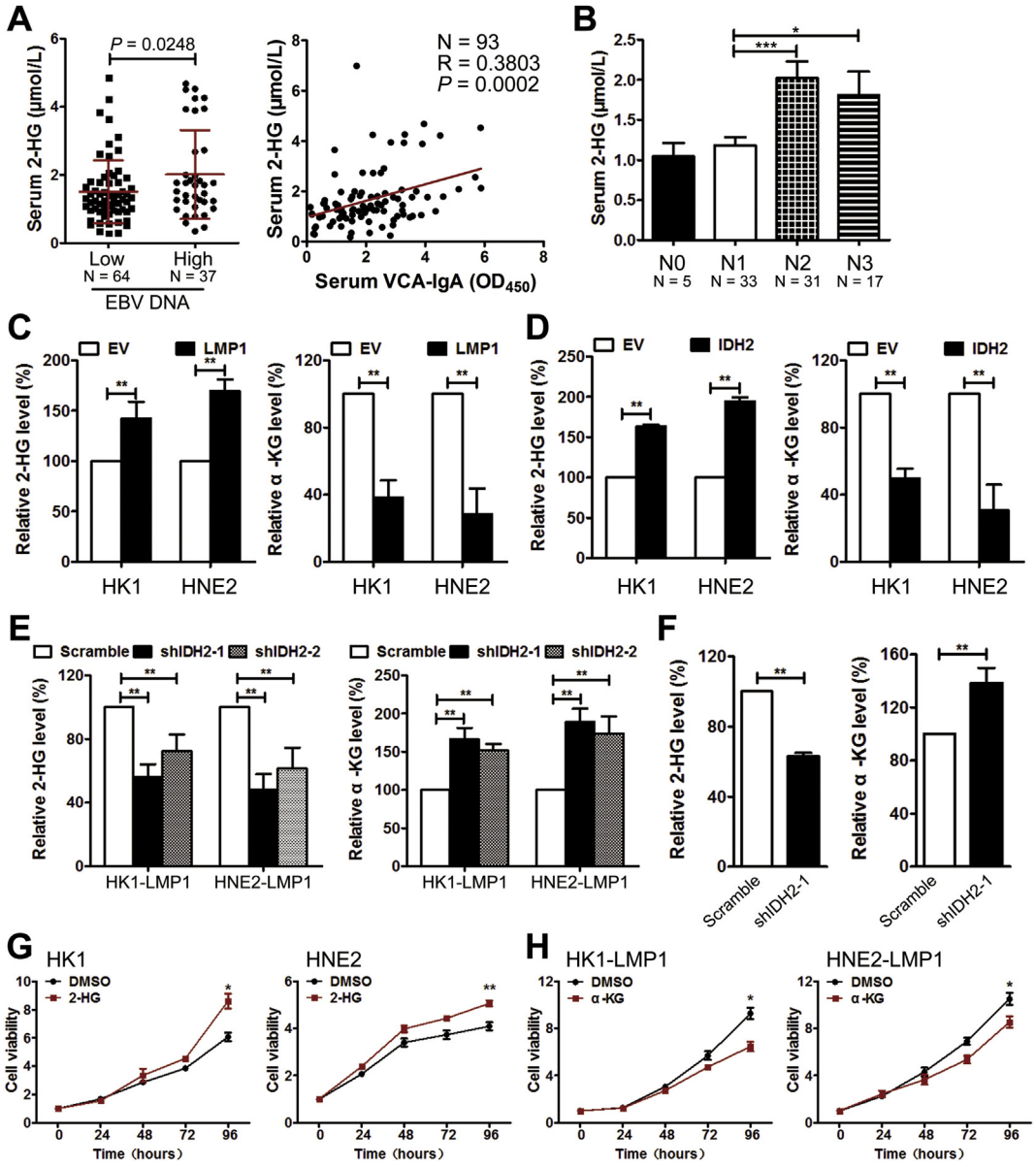

Figure 4: Overexpression of wild-type IDH2 is responsible for EBV-LMP1-modulated metabolic changes. A, the patients were divided into two groups based on their serum EBV DNA copy number: 1) low-level group = EBV DNA $\geq 1 \times 10^3$ copies and 2) high-level group = EBV DNA$<1 \times 10^3$ copies. Serum 2-HG levels were compared between the two groups *(left)*. The correlation between serum 2-HG levels and VCA-IgA levels was analyzed *(right)*. B, serum 2-HG levels were compared among different stages of regional lymph node metastases N stage. The levels of 2-HG *(left)* and α-KG *(right)* were measured in C, NPC cells transfected with empty or LMP1 expressing vector, D, in NPC cells transfected with empty or IDH2 expressing vector, in E, NPC cells transfected with scramble or IDH2 shRNAs, and in F, xenograft tissues from mice inoculated with HNE2-LMP1 cells transfected with scramble or IDH2 shRNA-1. Viability was measured by MTS in cells treated with G, DMSO/1 mM octyl-2-HG, and H, cells treated with DMSO/1 mM octyl-α-KG. Data are presented as means ± S.D.; *, $p < 0.05$; **, $p < 0.01$; ***, $p < 0.001$.

vital metabolic enzymes. The metabolic reprogramming induced by EBV infection usually leads to carcinogenesis [8,10,23].

2-HG is well-known to accumulate in IDH1/2-mutant cells. Recently, high levels of 2-HG were also observed in the absence of IDH1/2 mutations [7,24,25]. In breast cancer cells, alcohol dehydrogenase iron-containing protein 1 (ADHFE1) and c-Myc signaling were reported to contribute to 2-HG accumulation independent of IDHs [25,26]. The serine pathway enzyme phosphoglycerate dehydrogenase (PHGDH) catalyzes α-KG to 2-HG through an additional enzymatic activity [27]. Wild-type IDH2 also plays roles in 2-HG production, and metabolic flux analysis demonstrated that 2-HG is a byproduct of wild-type IDH2 [7,28–30]. Consistent with these studies, in this study we provided additional evidence showing that EBV-LMP1 consumes intracellular α-KG and produces 2-HG mediated through wild-type IDH2.

As an analog of α-KG, 2-HG inhibits α-KG-dependent dioxygenases, including ten-eleven translocation methylcytosine dioxygenases (TETs) and histone lysine demethylases (KDMs), and induces a hypermethylation phenotype in IDH-mutant cancers [31]. Intracellular 2-HG was reported to accumulate to more than 100-fold in IDH-

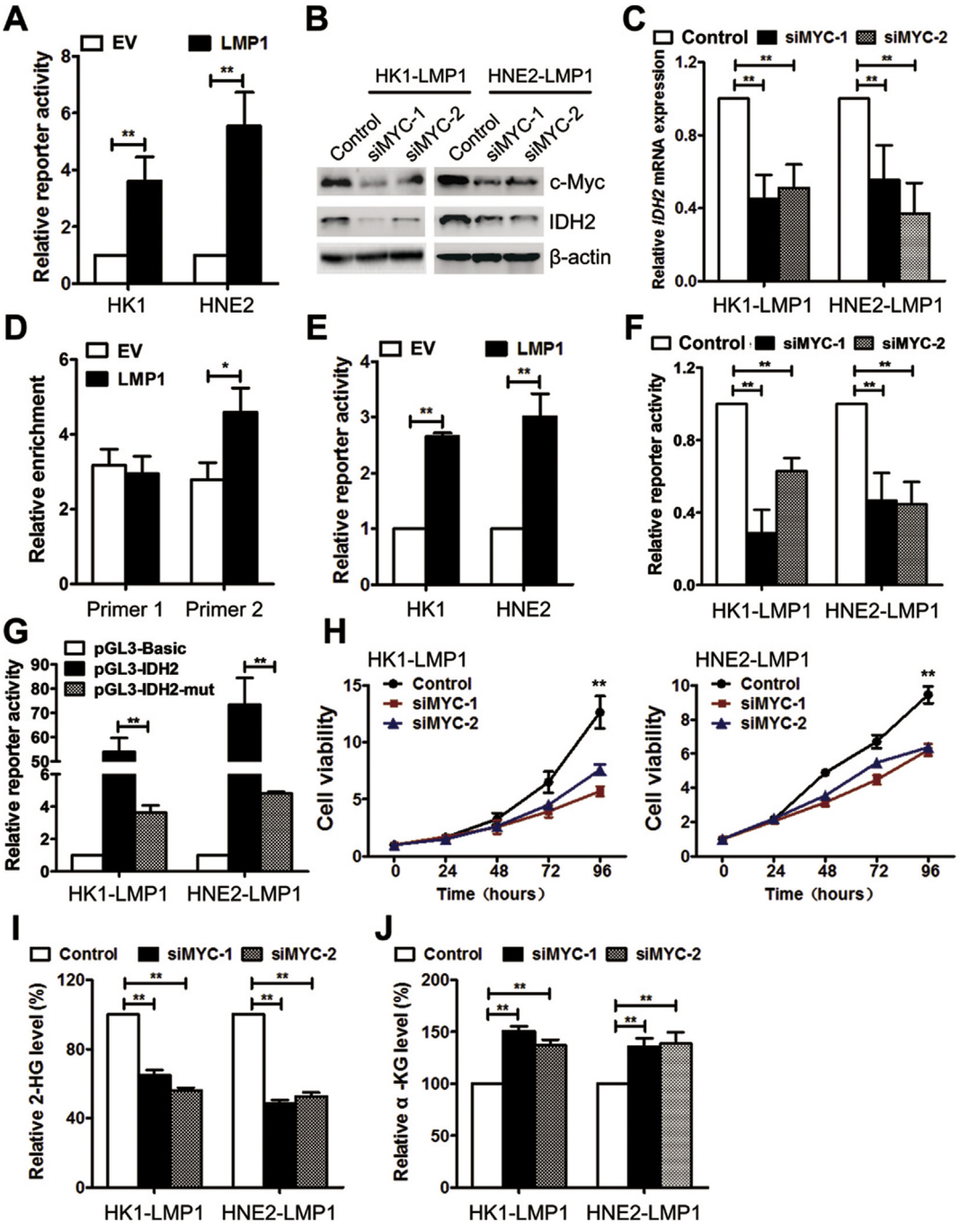

Figure 5: EBV-LMP1 facilitates IDH2 transcription through c-Myc. A, Myc-TA-luc and pRL-TK plasmids were co-transfected into NPC cells. The transcriptional activity of c-Myc was determined by the dual luciferase reporter assay. B, c-Myc and IDH2 protein expression was detected by western blot analysis in cells transfected with control or c-Myc siRNAs. C, *IDH2* mRNA expression was measured by RT-PCR. D, ChIP analysis was used to detect the presence of c-Myc in the promoter region of IDH2 by using two primer sites. E, pGL3-IDH2 and pRL-TK plasmids were co-transfected into NPC cells. IDH2 promoter activity was determined by the dual luciferase reporter assay. F, IDH2 promoter activity was determined in cells transfected with control or c-Myc siRNAs. G, luciferase activity was determined in cells transfected with pGL3-Basic, pGL3-IDH2, and pGL3-IDH2-mut (deletion of the c-Myc-binding site from −1446 to −1437 bp in pGL3-IDH2). H, viability was measured in cells transfected with control or c-Myc siRNAs by using MTS. The levels of I, 2-HG and J, α-KG (J) were measured in NPC cells transfected with control or c-Myc siRNAs. Data are presented as means ± S.D.; *, $p < 0.05$; **, $p < 0.01$.

mutant tumors, whereas wild-type IDH2 only modestly increased 2-HG levels [28]. EBV infection is a recognized epigenetic driver of tumorigenesis, and also a key regulator of metabolic reprogramming. We recently showed that fumarate accumulation and α-KG reduction induced by EBV-LMP1 participates in DNA methylation modification [10]. In the present study, EBV-LMP1 induced 2-HG accumulation and α-KG reduction by wild-type IDH2. However, the 2-HG level increased only modestly, suggesting that it might not be the only

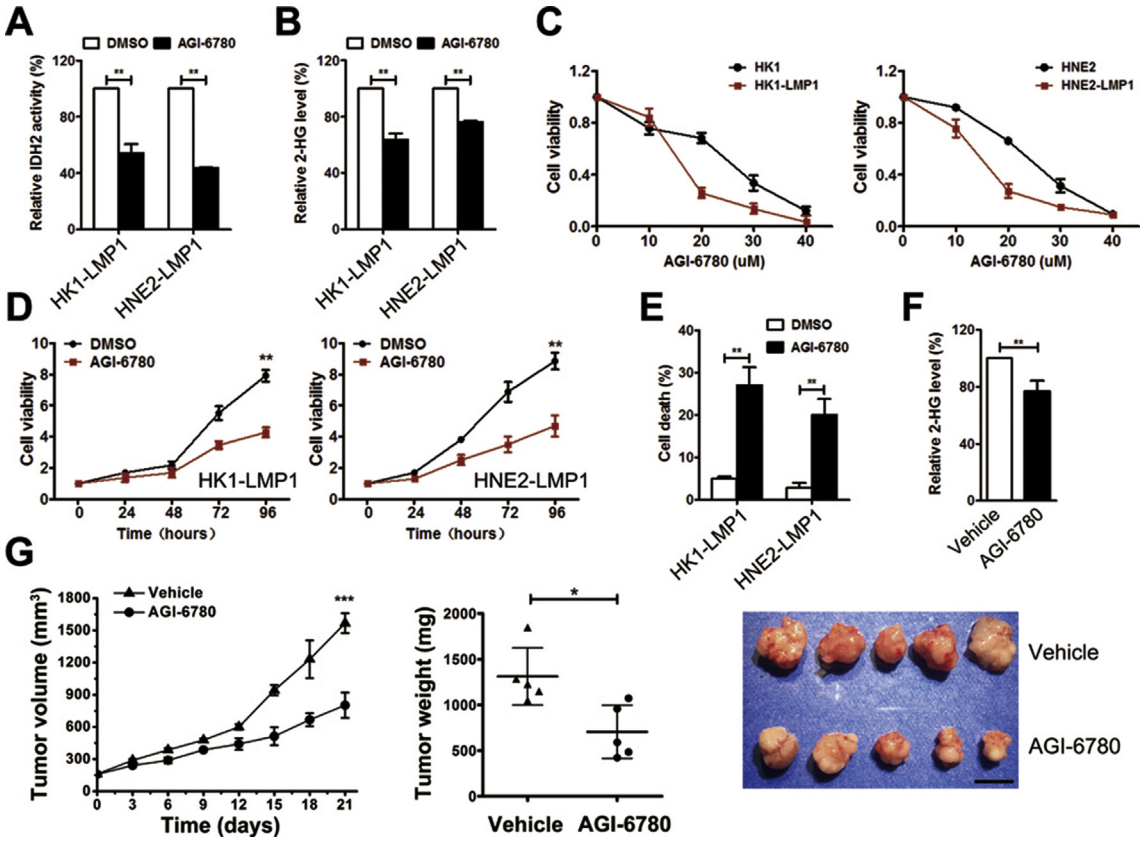

Figure 6: Targeting wild-type IDH2 inhibits cell viability and tumor growth. A, IDH activity and B, 2-HG levels were examined in NPC cells treated with DMSO/20 μM AGI-6780 for 24 h. C, viability was measured by MTS in cells treated with different concentrations of AGI-6780 (0—40 μM) for 48 h. D, viability was measured in cells treated with DMSO/10 μM AGI-6780. E, cell death was measured by Sytox Green staining in cells treated with DMSO/10 μM AGI-6780 for 48 h. F, levels of 2-HG were measured in xenograft tissues from mice inoculated with HNE2-LMP1 cells treated with corn oil (vehicle)/AGI-6780 (150 mg/kg). G, tumor volume (*left*) and tumor weight (*middle*) were measured in xenografts from mice inoculated with HNE2-LMP1 cells treated with vehicle/AGI-6780 (N = 5). Photographs of xenograft tumors are shown (*right*, scale bar = 1 cm). Data are presented as means ± S.D.; *, $p < 0.05$; **, $p < 0.01$; ***, $p < 0.001$.

factor. EBV-induced tumorigenesis could be caused by a series of metabolite changes. Overall, these findings might help us to understand cancer cell-directed effects of EBV-LMP1-induced metabolic reprogramming.

Interestingly, high levels of 2-HG were found in serum from patients with NPC with high serum EBV DNA levels, which suggests that EBV could promote the release of 2-HG into the extracellular space. The present study also showed a significant positive correlation between serum 2-HG levels and regional lymph node metastases of NPC, suggesting that EBV-infected cell-derived 2-HG may facilitate metastasis. Recent studies have confirmed the immunosuppressive effects of 2-HG [32—34]. The immunosuppressive microenvironment provides EBV with the opportunity for its latent infection and replication, which also favors tumor progression. Moreover, 2-HG has been reported to increase tumor angiogenesis, which is a key step in tumor metastasis [35]. The angiogenic activity induced by 2-HG might be responsible for NPC metastasis. Accordingly, EBV-LMP1-induced metabolic reprogramming could probably remodel the microenvironment by affecting non-neoplastic cells, but this requires further investigation.

Over-expression of c-Myc, which contributes to metabolic reprogramming essential to sustain cancer cell survival and proliferation, has been observed in a majority of cancers. As a transcription factor, c-Myc regulates cellular metabolism by targeting genes involved in glucose, glutamine, nucleotide, and fatty acid metabolism [36,37]. We previously showed that EBV-LMP1 increased the stability of the c-Myc protein, and sequentially elevated the expression of hexokinase 2 (HK2), a rate-limiting enzyme of glycolysis [8]. In the present study we confirmed that c-Myc transcriptionally activated wild-type IDH2 in EBV-LMP1-positive NPC cells. Moreover, c-Myc contributed to 2-HG accumulation through ADHFE1 in breast cancer cells [6]. We now describe another mechanism for c-Myc-dependent 2-HG accumulation. Overall, c-Myc could be a crucial regulator of metabolism in EBV-LMP1-dependent tumorigenesis.

Targeting mutant IDH2 has been demonstrated as an effective strategy for IDH2-mutant cancer therapy [38]. Enasidenib/AG-221, a mutant IDH2-selective inhibitor, has been approved by the US Food and Drug Administration (FDA) for IDH2-mutant relapsed or refractory acute myeloid leukemia [39]. Recent studies suggested that wild-type IDH2 could also be an actionable target in IDH2 wild-type cancers. IDH2 silencing decreased proliferation of human esophageal squamous cell cancer, thyroid carcinoma, colorectal cancer, and lung cancer cell lines [7,40—42]. The IDH2-specific inhibitor AGI-6780 could target both mutant and wild-type IDH2 [43]. Suppression of IDH2 by AGI-6780 enhanced the therapeutic efficacy of proteasome inhibitors in IDH2 wild-type hematological malignancies [44]. AGI-6780 alone decreased lung cancer cell survival in a time- and dose-dependent manner [7]. In the present study, targeting IDH2 decreased *in vitro* and *in vivo* survival of EBV-LMP1-positive tumor cells. Therefore, these findings highlight the important potential of wild-type IDH2 as a therapeutic target.

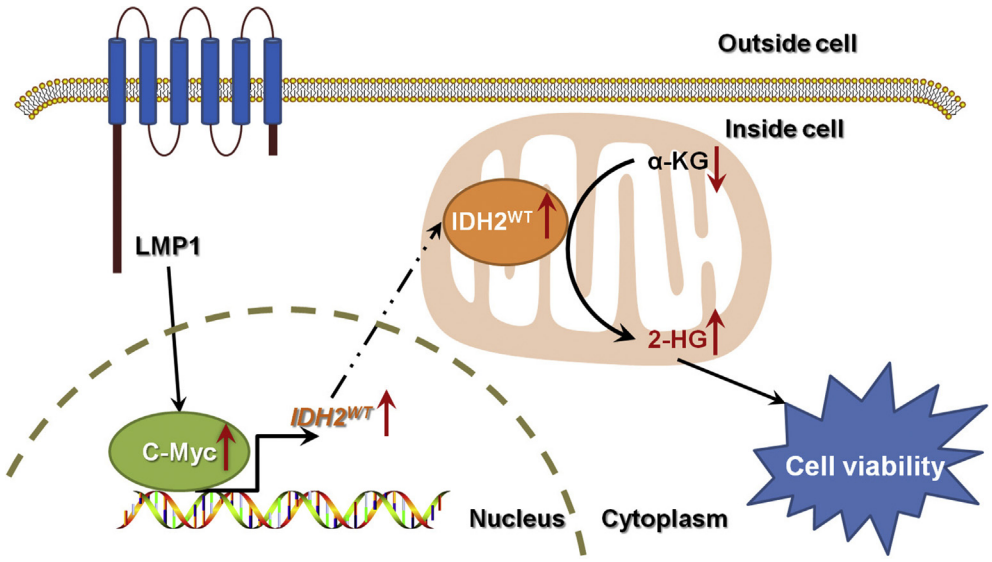

Figure 7: The EBV-LMP1/c-Myc/IDH2^{WT} signaling axis is critical for EBV-LMP1—dependent metabolic changes and tumorigenesis.

In summary, we identified that the EBV-LMP1/c-Myc/IDH2^{WT} signaling axis is critical for EBV-dependent metabolic changes and tumorigenesis (Figure 7). This study improves our understanding of infection-related carcinogenesis, shedding light on the link between EBV-infection, metabolic changes, and carcinogenesis. Further investigation of EBV-LMP1-induced metabolic reprogramming may provide new insights into EBV-related cancer diagnosis and therapy.

AUTHOR CONTRIBUTIONS

Conceptualization, F.S. and Y.H.; Investigation, Y.H., M.T., Y.L., L.X., L.Z., J.H., X.L., M.Z. and N.L.; Resources, J.F., J.Z., Q.G., S.Q., W.W., X.Z. and W.J., Writing- Original Draft, F.S., Writing- Review & Editing, F.S., A.M.B. and Y.C., Funding Acquisition, F.S. and Y.C., Supervision, Y.C. All authors read and approved the final manuscript.

ACKNOWLEDGMENTS

This study was supported by National Natural Science Foundation of China (81430064, 81602402, 81874172) and Hunan Provincial Natural Science Foundation of China (2018JJ3700).

CONFLICT OF INTEREST

None declared.

ABBREVIATIONS

α-KG	α-ketoglutarate
2-HG	2-hydroxyglutarate
EBV	Epstein—Barr virus
EBV-LMP1	EBV-encoded latent membrane protein 1
HNSCC	head and neck squamous cell carcinoma
HK2	hexokinase 2
IDH2	isocitrate dehydrogenase 2
IHC	immunohistochemistry
KDM	histone lysine demethylase
NP	nasopharyngitis
NPC	nasopharyngeal carcinoma
PHGDH	phosphoglycerate dehydrogenase
TCA cycle	tricarboxylic acid cycle
TET	ten-eleven translocation methylcytosine dioxygenase
VCA-IgA	IgA antibody against EBV viral capsid antigen

APPENDIX A. SUPPLEMENTARY DATA

Supplementary data to this article can be found online at https://doi.org/10.1016/j.molmet.2020.02.009.

REFERENCES

[1] Plummer, M., de Martel, C., Vignat, J., Ferlay, J., Bray, F., Franceschi, S., 2016. Global burden of cancers attributable to infections in 2012: a synthetic analysis. Lancet Global Health 4(9):e609—e616.

[2] Khan, G., Hashim, M.J., 2014. Global burden of deaths from Epstein-Barr virus attributable malignancies 1990-2010. Infectious Agents and Cancer 9(1):38.

[3] Cao, Y., 2017. EBV based cancer prevention and therapy in nasopharyngeal carcinoma. NPJ Precision Oncology 1(1):10.

[4] Tsao, S.W., Tsang, C.M., To, K.F., Lo, K.W., 2015. The role of Epstein-Barr virus in epithelial malignancies. The Journal of Pathology 235(2):323—333.

[5] Yang, H., Ye, D., Guan, K.L., Xiong, Y., 2012. IDH1 and IDH2 mutations in tumorigenesis: mechanistic insights and clinical perspectives. Clinical Cancer Research 18(20):5562—5571.

[6] Bergaggio, E., Piva, R., 2019. Wild-type IDH enzymes as actionable targets for cancer therapy. Cancers (Basel) 11(4).

[7] Li, J., He, Y., Tan, Z., Lu, J., Li, L., Song, X., et al., 2018. Wild-type IDH2 promotes the Warburg effect and tumor growth through HIF1alpha in lung cancer. Theranostics 8(15):4050—4061.

[8] Xiao, L., Hu, Z.Y., Dong, X., Tan, Z., Li, W., Tang, M., et al., 2014. Targeting Epstein-Barr virus oncoprotein LMP1-mediated glycolysis sensitizes nasopharyngeal carcinoma to radiation therapy. Oncogene 33(37):4568—4578.

[9] Lu, J., Tang, M., Li, H., Xu, Z., Weng, X., Li, J., et al., 2016. EBV-LMP1 suppresses the DNA damage response through DNA-PK/AMPK signaling to promote radioresistance in nasopharyngeal carcinoma. Cancer Letters 380(1):191—200.

[10] Shi, F., Zhou, M., Shang, L., Du, Q., Li, Y., Xie, L., et al., 2019. EBV(LMP1)-induced metabolic reprogramming inhibits necroptosis through the hypermethylation of the RIP3 promoter. Theranostics 9(9):2424—2437.
[11] Lo, A.K., Dawson, C.W., Young, L.S., Lo, K.W., 2017. The role of metabolic reprogramming in gamma-herpesvirus-associated oncogenesis. International Journal of Cancer 141(8):1512—1521.
[12] Zheng, X.H., Lu, L.X., Li, X.Z., Jia, W.H., 2015. Quantification of Epstein-Barr virus DNA load in nasopharyngeal brushing samples in the diagnosis of nasopharyngeal carcinoma in southern China. Cancer Science 106(9):1196—1201.
[13] Shi, Y., Tao, Y., Jiang, Y., Xu, Y., Yan, B., Chen, X., et al., 2012. Nuclear epidermal growth factor receptor interacts with transcriptional intermediary factor 2 to activate cyclin D1 gene expression triggered by the oncoprotein latent membrane protein 1. Carcinogenesis 33(8):1468—1478.
[14] Liu, X., Li, Y., Peng, S., Yu, X., Li, W., Shi, F., et al., 2018. Epstein-Barr virus encoded latent membrane protein 1 suppresses necroptosis through targeting RIPK1/3 ubiquitination. Cell Death & Disease 9(2):53.
[15] Shi, F., Shang, L., Pan, B.Q., Wang, X.M., Jiang, Y.Y., Hao, J.J., et al., 2014. Calreticulin promotes migration and invasion of esophageal cancer cells by upregulating neuropilin-1 expression via STAT5A. Clinical Cancer Research 20(23):6153—6162.
[16] Hau, P.M., Tsang, C.M., Yip, Y.L., Huen, M.S., Tsao, S.W., 2011. Id1 interacts and stabilizes the Epstein-Barr virus latent membrane protein 1 (LMP1) in nasopharyngeal epithelial cells. PloS One 6(6):e21176.
[17] Shi, F., Shang, L., Yang, L.Y., Jiang, Y.Y., Wang, X.M., Hao, J.J., et al., 2018. Neuropilin-1 contributes to esophageal squamous cancer progression via promoting P65-dependent cell proliferation. Oncogene 37(7):935—943.
[18] Du, Q., Tan, Z., Shi, F., Tang, M., Xie, L., Zhao, L., et al., 2019. PGC1alpha/CEBPB/CPT1A axis promotes radiation resistance of nasopharyngeal carcinoma through activating fatty acid oxidation. Cancer Science 110(6):2050—2062.
[19] Faqing, T., Zhi, H., Liqun, Y., Min, T., Huanhua, G., Xiyun, D., et al., 2005. Epstein-Barr virus LMP1 initiates cell proliferation and apoptosis inhibition via regulating expression of Survivin in nasopharyngeal carcinoma. Experimental Oncology 27(2):96—101.
[20] Tao, Y., Shi, Y., Jia, J., Jiang, Y., Yang, L., Cao, Y., 2015. Novel roles and therapeutic targets of Epstein-Barr virus-encoded latent membrane protein 1-induced oncogenesis in nasopharyngeal carcinoma. Expert Reviews in Molecular Medicine 17:e15.
[21] Sanchez, E.L., Lagunoff, M., 2015. Viral activation of cellular metabolism. Virology 479—480:609—618.
[22] Levy, P., Bartosch, B., 2016. Metabolic reprogramming: a hallmark of viral oncogenesis. Oncogene 35(32):4155—4164.
[23] Luo, X., Hong, L., Cheng, C., Li, N., Zhao, X., Shi, F., et al., 2018. DNMT1 mediates metabolic reprogramming induced by Epstein-Barr virus latent membrane protein 1 and reversed by grifolin in nasopharyngeal carcinoma. Cell Death & Disease 9(6):619.
[24] Miyake, K., Baba, Y., Ishimoto, T., Hiyoshi, Y., Iwatsuki, M., Miyamoto, Y., et al., 2018. Isocitrate dehydrogenase gene mutations and 2-hydroxyglutarate accumulation in esophageal squamous cell carcinoma. Medical Oncology 36(1):11.
[25] Terunuma, A., Putluri, N., Mishra, P., Mathe, E.A., Dorsey, T.H., Yi, M., et al., 2014. MYC-driven accumulation of 2-hydroxyglutarate is associated with breast cancer prognosis. Journal of Clinical Investigation 124(1):398—412.
[26] Mishra, P., Tang, W., Putluri, V., Dorsey, T.H., Jin, F., Wang, F., et al., 2018. ADHFE1 is a breast cancer oncogene and induces metabolic reprogramming. Journal of Clinical Investigation 128(1):323—340.
[27] Fan, J., Teng, X., Liu, L., Mattaini, K.R., Looper, R.E., Vander Heiden, M.G., et al., 2015. Human phosphoglycerate dehydrogenase produces the oncometabolite D-2-hydroxyglutarate. ACS Chemical Biology 10(2):510—516.
[28] Matsunaga, H., Futakuchi-Tsuchida, A., Takahashi, M., Ishikawa, T., Tsuji, M., Ando, O., 2012. IDH1 and IDH2 have critical roles in 2-hydroxyglutarate production in D-2-hydroxyglutarate dehydrogenase depleted cells. Biochemical and Biophysical Research Communications 423(3):553—556.
[29] Smolkova, K., Dvorak, A., Zelenka, J., Vitek, L., Jezek, P., 2015. Reductive carboxylation and 2-hydroxyglutarate formation by wild-type IDH2 in breast carcinoma cells. The International Journal of Biochemistry & Cell Biology 65:125—133.
[30] Wise, D.R., Ward, P.S., Shay, J.E., Cross, J.R., Gruber, J.J., Sachdeva, U.M., et al., 2011. Hypoxia promotes isocitrate dehydrogenase-dependent carboxylation of alpha-ketoglutarate to citrate to support cell growth and viability. Proceedings of the National Academy of Sciences of the U S A 108(49):19611—19616.
[31] Dang, L., Su, S.M., 2017. Isocitrate dehydrogenase mutation and (R)-2-Hydroxyglutarate: from basic discovery to therapeutics development. Annual Review of Biochemistry 86:305—331.
[32] Galluzzi, L., Kroemer, G., 2018. Potent immunosuppressive effects of the oncometabolite R-2-hydroxyglutarate. OncoImmunology 7(12):e1528815.
[33] Bunse, L., Pusch, S., Bunse, T., Sahm, F., Sanghvi, K., Friedrich, M., et al., 2018. Suppression of antitumor T cell immunity by the oncometabolite (R)-2-hydroxyglutarate. Nature Medicine 24(8):1192—1203.
[34] Zhang, L., Sorensen, M.D., Kristensen, B.W., Reifenberger, G., McIntyre, T.M., Lin, F., 2018. D-2-Hydroxyglutarate is an intercellular mediator in IDH-mutant gliomas inhibiting complement and T cells. Clinical Cancer Research 24(21):5381—5391.
[35] Seok, J., Yoon, S.H., Lee, S.H., Jung, J.H., Lee, Y.M., 2019. The oncometabolite d2hydroxyglutarate induces angiogenic activity through the vascular endothelial growth factor receptor 2 signaling pathway. International Journal of Oncology 54(2):753—763.
[36] Stine, Z.E., Walton, Z.E., Altman, B.J., Hsieh, A.L., Dang, C.V., 2015. MYC, metabolism, and cancer. Cancer Discovery 5(10):1024—1039.
[37] Wahlstrom, T., Henriksson, M.A., 2015. Impact of MYC in regulation of tumor cell metabolism. Biochimica et Biophysica Acta 1849(5):563—569.
[38] Golub, D., Iyengar, N., Dogra, S., Wong, T., Bready, D., Tang, K., et al., 2019. Mutant isocitrate dehydrogenase inhibitors as targeted cancer therapeutics. Frontiers in Oncology 9:417.
[39] Kim, E.S., 2017. Enasidenib: first global approval. Drugs 77(15):1705—1711.
[40] Lv, Q., Xing, S., Li, Z., Li, J., Gong, P., Xu, X., et al., 2012. Altered expression levels of IDH2 are involved in the development of colon cancer. Experimental and Therapeutic Medicine 4(5):801—806.
[41] Chen, X., Xu, W., Wang, C., Liu, F., Guan, S., Sun, Y., et al., 2017. The clinical significance of isocitrate dehydrogenase 2 in esophageal squamous cell carcinoma. American Journal of Cancer Research 7(3):700—714.
[42] Zhang, J., Hu, L., Wang, H., Zhi, J., Hou, X., Wu, Y., et al., 2019. Functional analysis and clinical significance of the isocitrate dehydrogenase 2 gene in papillary thyroid carcinoma. Cancer Management and Research 11:3765—3777.
[43] Wang, F., Travins, J., DeLaBarre, B., Penard-Lacronique, V., Schalm, S., Hansen, E., et al., 2013. Targeted inhibition of mutant IDH2 in leukemia cells induces cellular differentiation. Science 340(6132):622—626.
[44] Bergaggio, E., Riganti, C., Garaffo, G., Vitale, N., Mereu, E., Bandini, C., et al., 2019. IDH2 inhibition enhances proteasome inhibitor responsiveness in hematological malignancies. Blood 133(2):156—167.

